

Article

Space Charge Behavior in Paper Insulation Induced by Copper Sulfide in High-Voltage Direct Current Power Transformers

Ruijin Liao ^{1,*}, Ende Hu ¹, Lijun Yang ¹ and Yuan Yuan ²

¹ The State Key Laboratory of Power Transmission Equipment & System Security and New Technology, College of Electrical Engineering, Chongqing University, Chongqing 400044, China; E-Mails: zjhed@cqu.edu.cn (E.H.); yljcqu@cqu.edu.cn (L.Y.)

² The Department of Material Engineering, Chongqing University, Chongqing 400044, China; E-Mail: yuany@cqu.edu.cn

* Author to whom correspondence should be addressed; E-Mail: rjliao@cqu.edu.cn; Tel.: +86-23-6510-6880; Fax: +86-23-6510-2442.

Academic Editor: Paul Stewart

Received: 13 June 2015 / Accepted: 27 July 2015 / Published: 5 August 2015

Abstract: The main insulation system in high-voltage direct current (HVDC) transformer consists of oil-paper insulation. The formation of space charge in insulation paper is crucial for the dielectric strength. Unfortunately, space charge behavior changes because of the corrosive sulfur substance in oil. This paper presents the space charge behavior in insulation paper induced by copper sulfide generated by corrosive sulfur in insulation oil. Thermal aging tests of paper-wrapped copper strip called the pigtail model were conducted at 130 °C in laboratory. Scanning electron microscopy (SEM) was used to observe the surface of copper and paper. Pulse electroacoustic (PEA) and thermally stimulated current (TSC) methods were used to obtain the space charge behavior in paper. Results showed that both maximum and total amount of space charge increased for the insulation paper contaminated by semi-conductor chemical substance copper sulfide. The space charge decay rate of contaminated paper was significantly enhanced after the polarization voltage was removed. The TSC results revealed that copper sulfide increased the trap density and lowered the shallow trap energy levels. These results contributed to charge transportation by de-trapping and trapping processes. This improved charge transportation could be the main reason for the decreased breakdown voltage of paper insulation material.

Keywords: corrosive sulfur; pulse electroacoustic (PEA); stimulated current (TSC); scanning electron microscopy (SEM); copper sulfide; thermal aging; oil-paper; high-voltage direct (HVDC) transformer

1. Introduction

Oil-paper is widely used as an insulating medium in various high voltage apparatuses, such as power transformers, capacitors, and HVDC devices, which play a vital role in electrical power networks [1,2]. Aging of oil-paper can eventually threaten the safe operation of electrical devices. The space charge will accumulate within the paper materials under the action of DC high voltage, leading to the distortion of internal local electrical field distribution [3,4]. Therefore, the aging speed of paper material is accelerated. Unfortunately, researchers have recently faced a new problem, namely, corrosive sulfur in insulating oil. Corrosive sulfur can form the semi-conductor substance copper sulfide, which will be deposited on the paper surface [5,6]. Insulating resistance and dielectric property of oil-paper insulation have decreased because of emergence of this substance. The understanding of space charge behavior in paper contaminated by copper sulfide is of significant interests.

The sources of corrosive sulfur in oil have not yet been completely identified, but the indications suggest that they are the residuals of the refining process [7]. The emergence of copper sulfide by-product caused by the chemical reaction between corrosive sulfur (mainly dibenzyl disulfide DBDS) in the insulation oil and copper conductor greatly change the dielectric characteristic of paper. The deposition of copper sulfide on the paper surface distorts the electric field, decreases the insulating resistance, and accelerates the aging of insulating materials or even causes direct breakdown [5,8].

The space charge behavior of aged oil is complicated because of the formation of polar substances such as water, acid, and organic molecules. The processes of charge injection, migration, and decay in paper material are directly influenced by these substances. However, to date, knowledge about the relationship between the copper sulfide deposition on paper and space charge behavior is still lacking. On the other hand, distorted electric field caused by the copper sulfide deposition plays a vital role in the decreasing breakdown voltage of insulation paper [9]. However, to the authors' knowledge, space charge behavior is likely to be one of the most fundamental reasons for the characteristic change in paper material. The insulation risk caused by copper sulfide from the perspective of micros should be determined. Thus, in this paper, we aimed to understand the effect of copper sulfide on the space charge behavior of accelerated thermal aging paper material, and analyze the failure of paper material caused by copper sulfide deposition.

2. Experiments

Selected corrosive sulfur DBDS was purchased from a local company. The insulation oil used in this experiment was 25# mineral oil without any corrosive sulfur or DBDS substance. The corrosivity of the oil was based on the procedures stipulated by IEC62535. Table 1 shows the typical properties of this 25# commercially available insulation oil.

Three oil samples were prepared: one was base oil (called sample I), which had no corrosive sulfur or DBDS. The second oil sample was called sample II, in which 500 ppm DBDS was added. The third oil sample was called sample III, in which 1000 ppm DBDS was added. Three oil samples with different DBDS concentrations were prepared. Paper-wrapped copper windings and these oil samples were dried at 90 °C/50 Pa and then finished the oil impregnation [10]. Windings and oil samples were thermally aged for 24 days at 130 °C to obtain three paper samples. One aged paper was uncontaminated by copper sulfide deposition, whereas the other two were contaminated by copper sulfide deposition with different levels of severity. The detailed information is listed in Table 2.

Table 1. Properties of tested mineral base insulation oil.

Characteristics	Items	Properties
Function	Density (20 °C), kg/m ³	883.2
	Viscosity (40 °C), mm ² /s	9.67
	Viscosity(−20 °C), mm ² /s	488.9
	Breakdown voltage, kV	62
Stability	Acidity, mg KOH/g	0.008
	Corrosivity	None

Table 2. Testing samples and condition of thermal aging tests.

Specimen	Description	Dibenzyl disulfide (DBDS) concentration (mg/kg)	Temperature (°C)
Sample 1	Oil + winding	0	130
Sample 2	Oil + winding + DBDS	500	130
Sample 3	Oil + winding + DBDS	1000	130

The paper-wrapped copper windings were provided by Chongqing ABB Transformer Co., Ltd. (Chongqing, China). Figure 1a shows the winding, and copper strip is wrapped by insulation paper. The windings were processed to pig-tail model and each model consists of two windings, the dimension of this model is shown in Figure 1b. The length of the winding is 75.00 mm and the tail at the end of winding is 15.00 mm.

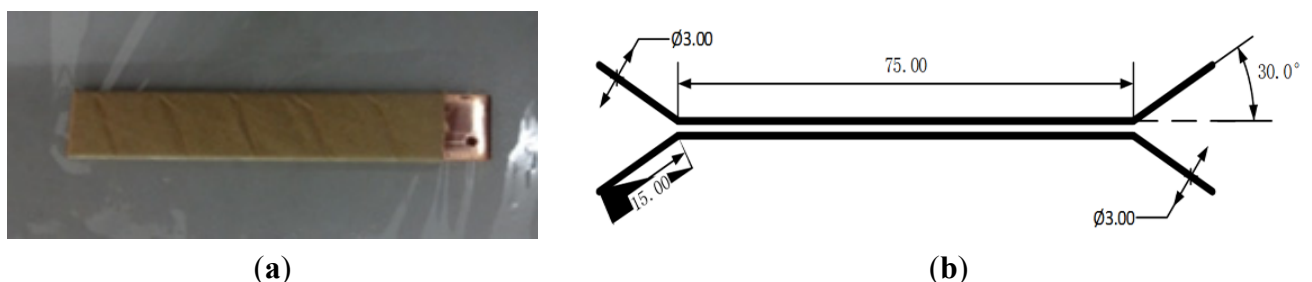


Figure 1. Paper-wrapped copper winding and dimension pig-tail model. (a) winding; (b) dimension of pig-tail model.

The alternating current (AC) breakdown voltage of oil samples was obtained according to the IEC 60156 standard. Partial discharge inception voltages (PDIV) of oil-impregnated papers were measured based on the pig-tail model shown in Figure 1b. One of the windings in the pig-tail model was connected with high voltage supply (AC) through the hole, which was located in the end of the winding, and

another winding was connected with the ground electrode. The pig-tail model was immersed in insulation oil during the PD test.

Scanning electron microscopy (SEM) was used to analyze the deposition on the paper surface. The space charge behaviors in paper materials were measured by PEA method based on previous studies [11,12]. Trap characteristics of paper samples were tested using TSC method. The setup and operating procedure of PEA and TSC are described in detail in previous publications [13].

3. Results

3.1. Appearance of Copper Strip and Paper

The comparison of three samples, including the appearance of copper and paper surface, is shown in Figure 2. No deposition was formed on the paper surface in sample I, as shown in Figure 2a. The paper surface was clear without any contamination. However, some silvery white deposition could be clearly observed in Figure 2b. The copper surface became darker compared with that in Figure 2a, and some parts of the paper surface were covered by deposition. For sample III (Figure 2c), the surface copper became darker than the former two copper samples. The whole surface of paper was covered by deposition.

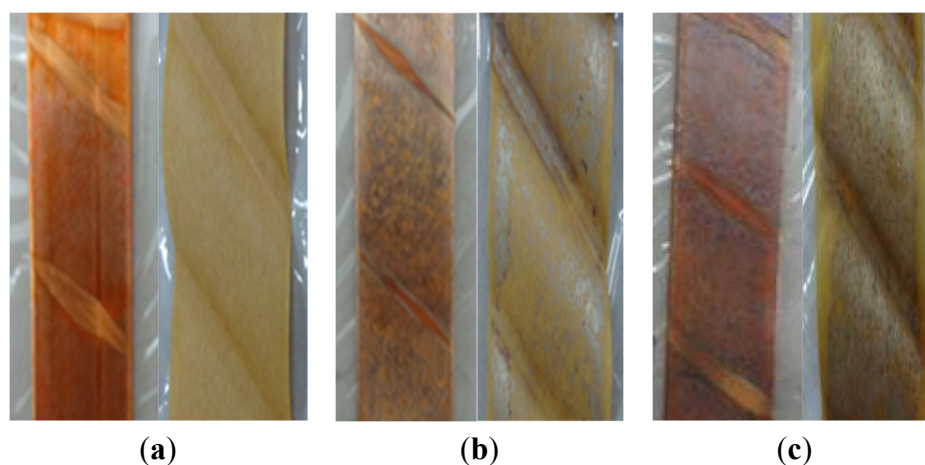


Figure 2. Appearance of copper and paper surface of samples (a) sample I; (b) sample II; and (c) sample III.

3.2. Scanning Electron Microscopy (SEM) of Copper Strips and Paper

SEM images of the three copper strip samples are shown in Figure 3. Lines were clear on the copper surface in sample I, as shown in Figure 3. The copper strip had a flat surface without bulges. The surface of the copper strip of sample II, which was contaminated by corrosive sulfur, became rough and numerous granular sediments were present on the copper surface. White particles appeared and lines were covered by particles. Nevertheless, the contamination condition in sample III was the most serious one. The SEM images of the three paper samples at a magnification of hundreds of times (10 μm) are shown in Figure 3. The fiber texture of paper was clearly visible in paper sample I. By contrast, the fiber texture of paper sample II was not easy to visualize, because deposition appeared on the paper surface. This appearance became fuzzy and more serious in paper sample III. The gaps between fibers were filled with white particles and some fibers were covered by particles.

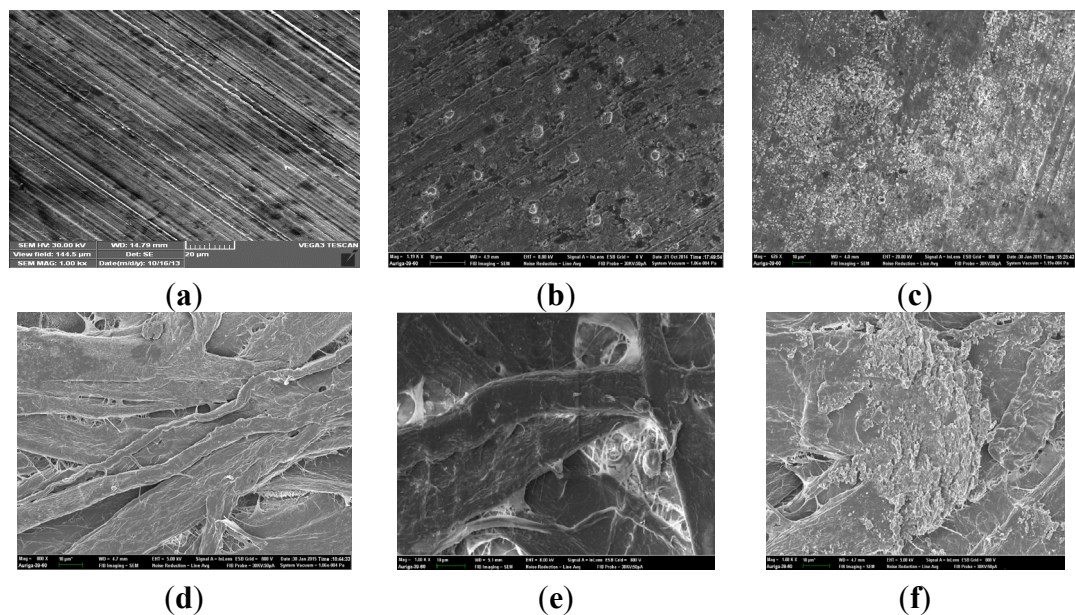


Figure 3. Scanning electron microscopy (SEM) of copper strip surface: (a) Sample I; (b) Sample II; (c) Sample III and paper surface: (d) Sample I; (e) Sample II; (f) Sample III.

3.3. Electrical Properties of Insulation Paper

Most studies have proven that the deposition on the copper surface and paper surface is copper sulfide substance (mainly Cu_2S) [14]. The electrical properties of the paper material changed because of the emergence of this kind of substance as result of its semi-conductive nature [15]. SEM and energy dispersive X-ray (EDX) spectrum were used to analyze this substance, and the results are shown in Figure 4 (working distance was kept at $1\text{ }\mu\text{m}$, magnification = $4.66\text{ K}\times$). As shown in Figure 4a, the copper surface was covered by a large number of granules, the element composition of which was confirmed by EDX (Figure 4b). Figure 4c shows that the atomic number between Cu and S was 39.70/11.22, which is close to 4:1 (Cu_2S :4:1). Another study [16] also pointed out that the deposition is mainly Cu_2S , which contains small amounts of CuO and CuS .

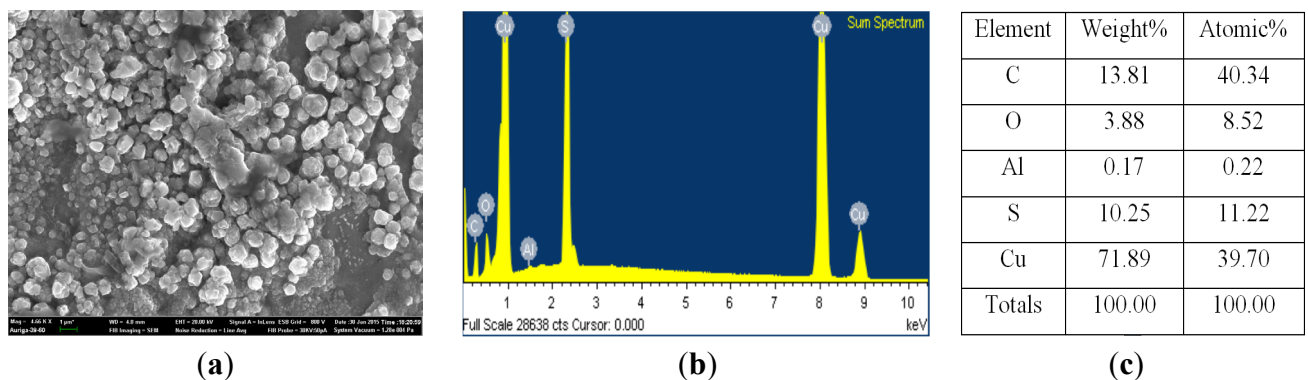


Figure 4. (a) SEM image; (b) energy dispersive X-ray (EDX) analysis; and (c) element composition of copper surface.

The breakdown strength of oil-impregnated paper wrapped copper winding with and without copper sulfide deposition is shown in Table 3. Compared with paper-wrapped copper winding of sample I,

the breakdown voltage of oil and PDIV of the winding of sample II decreased by 4.6% and 21.73%, respectively. Nevertheless, the degree of decrease for sample III was more obvious. The breakdown and partial discharge inception voltage of sample III decreased by 14.45% and 42.86%, respectively. The variation in breakdown voltage and PDIV indicated that the presence of copper sulfide on paper contributed to the decrease in electrical properties, and this contribution may be caused by the semi-conductor properties of copper sulfide.

Table 3. Deposition effects on electrical strength of oils and paper-wrapped copper winding. PDIV: partial discharge inception voltages.

Items	Parameter	Sample I	Sample II	Sample III
Oil	Breakdown voltage (kV)	49.8	47.5	42.6
	Standard deviation (kV)	3.14	3.62	3.29
Paper	Partial discharge (PD) inception voltage (kV)	16.1	12.6	9.2
	PD pico-coulomb of PDIV (pC)	209	610	725

3.4. Space Charge Behavior of Insulation Paper

The charge transport characteristic in insulation paper will change with the introduction of copper sulfide. The PEA method was used to obtain the space charge behavior in paper. After samples were subjected to a DC electric field, the space charge distribution in paper samples is shown in Figure 5.

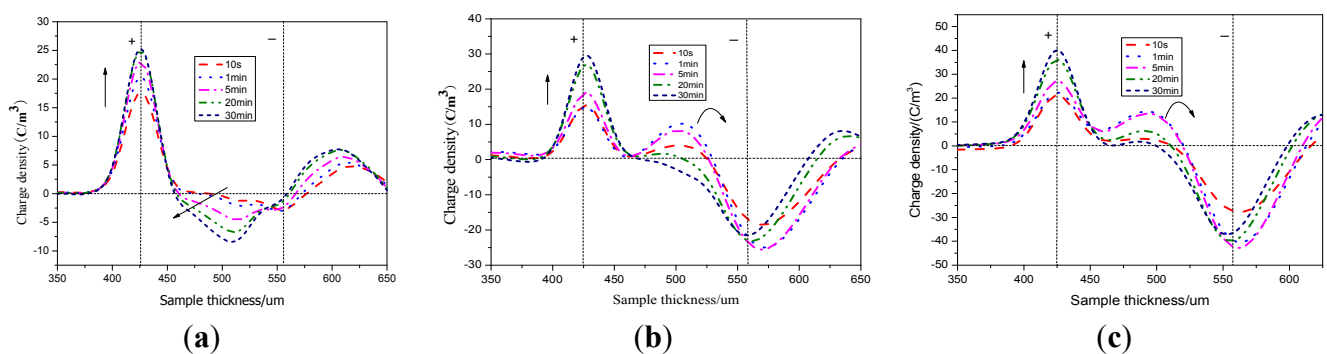


Figure 5. Volt-on space charge distribution of paper samples: (a) sample I; (b) sample II; and (c) sample III.

The anode peak was sharp and evident. As shown in Figure 5b, the peak at the anode electrode increased compared with that in Figure 5a. Copper sulfide deposition had a significant effect on the space charge behavior. The maximum space charge in paper sample II (Figure 5b: 29 C/m³) was higher than that of sample I (Figure 5a: 24 C/m³) when the same DC voltage was applied, implying that more charge carriers were formed in the paper contaminated by copper sulfide. The maximum space charge reached the highest value in sample III (Figure 5c: 40 C/m³). Notably, for oil-paper contaminated by copper sulfide deposition, the positive charge injection behavior was different from that of paper without contamination. For the oil/paper sample without contamination, negative charges were injected into the inside of paper (around 500 μm) immediately once an electric field was applied. The amount of negative charge from this injection increased as the electric field applied. Therefore, most charges inside paper (around 500 μm) were negative, as shown in Figure 5a. For sample II, not only negative but also positive

charge can be found inside of paper. A positive charge observed at the same position (500 μm) initially increased and then decreased after 1 min, as shown in Figure 5b. The positive charge bump increased, indicating that the positive charge injection was strengthened when paper was contaminated by copper sulfide. For sample III, a positive charge bump was found in the beginning of voltage application. However, the maximum positive charge density inside paper reached 15 C/m^3 , which was higher than that in sample II (10 C/m^3). Results in Figure 5 demonstrated that higher deposition in paper, resulting in a more obvious positive charge injection.

Figure 6 shows the space charge distribution measured after the removal of the applied voltage for oil-paper samples with different contents of copper sulfide deposition. The maximum space charge in contaminated paper around the anode (about -5.5 C/m^3 as shown in Figure 6b) was higher than that of uncontaminated paper (about -2.5 C/m^3 as shown in Figure 6a). Nevertheless, the maximum space charge in sample III was the highest (about -11 C/m^3 as shown in Figure 6c). For all paper samples, a majority of space charge in the bulk disappeared after 5 min. The space charge decay of sample II was 2.85-fold of that in sample I after the external electrical field was removed for 5 min. Thus, the deposition on the paper could enhance the dissipation mobility of the charges.

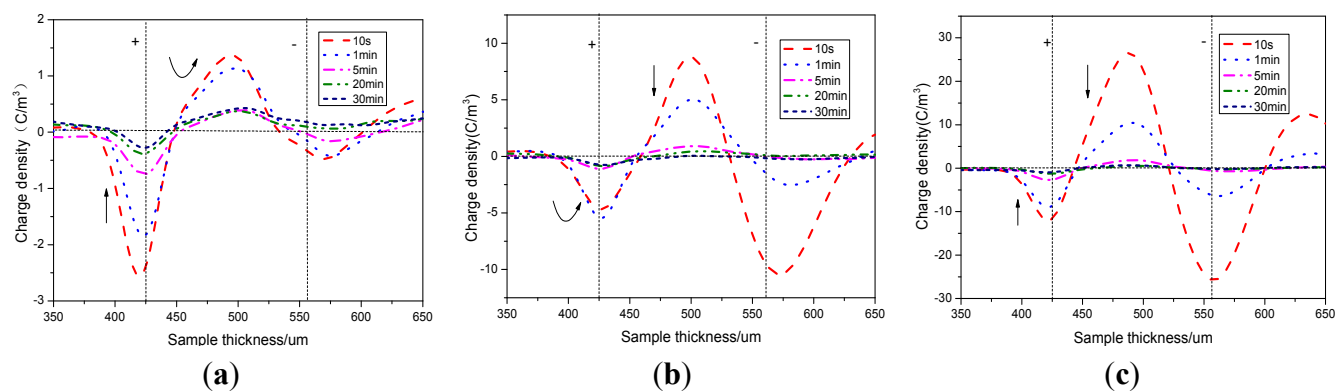


Figure 6. Volt-off space charge distribution of paper samples: (a) without contamination; (b) with contamination; and (c) with more contamination.

The decay speed of the three samples was determined using the following math model:

$$Q(t) = Q(0) + Ae^{-\frac{t}{\tau}} \quad (1)$$

where $Q(t)$ is space charge amount at time t , $Q(0)$ is the residual space charge amount when the decay is moving toward stability, and τ is the decay time constant. The relationship is shown in Table 4.

Table 4. Relationship between space charge amount and time for oil impregnated papers.

Sample	Formula	R-squared
I	$Q(t) = 72.3\exp(-t/4.1) + 27.5$	0.989
II	$Q(t) = 522.8\exp(-t/2.18) + 73.1$	0.985
III	$Q(t) = 1217.6\exp(-t/1.7) + 132.9$	0.971

The τ represents the decay speed of space charge. A low value τ results in higher decay speed of space charge. Thus, the space charge in contaminated paper had higher decay speed than that of uncontaminated paper.

4. Discussion

Copper sulfide deposition on paper exerted great effects on the electrical properties and space charge dynamics in oil-paper samples. The emergence of copper sulfide deposition on paper not only enhanced the charge accumulation but also improved the mobility of the charge in the samples. Oil-paper degradation caused by thermal aging is irreversible. The aging by-products deposited on the insulation paper cannot be removed. The decreased breakdown performance of sample II and sample III was largely attributed to the by-product copper sulfide (Cu_2S) because of the physical/chemical interaction between DBDS and copper, as shown in Figure 7 [14].

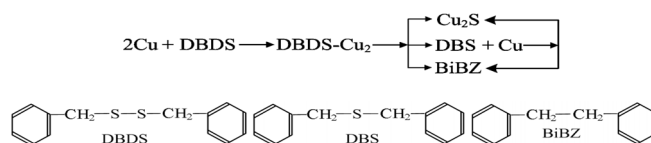


Figure 7. Chemical structure of dibenzyl disulfide (DBDS) and the reaction between DBDS and copper conductor.

DBDS, is a corrosive sulfur that can attack copper windings under certain conditions. The DBDS-Cu complex, which is soluble in oil, formed. Part of the DBDS-Cu complex remained on the copper surface and then decomposed into Cu_2S . Portions of the complex transferred from the copper surface to the paper surface through bulk oil. Copper sulfide eventually formed on the paper surface.

Copper sulfide deposition can not only deposit on the paper surface but also permeate into paper [17]. The distribution of the electric field was distorted because of this deposition and permeation, leading to the downtrend of PDIV and breakdown voltage [9]. The decreased PDIV and breakdown voltage was related to space charge behavior. However, space charge distribution and decay are associated with trapping/de-trapping processes and charge transport in insulation paper materials [18,19]. It was reported that high conductivity leads to the high mobility of the charges trapped in the samples [20]. The Cu_2S could enhance the dissipation mobility of the space charges and mobility of charges in insulation paper because of its conductive characteristic. The higher this substance content in insulation paper, the faster the trapped charge moves. Thus, the trap characteristics of two samples (uncontaminated paper and contaminated paper) were tested to further investigate the charge behavior, and the results are shown in Figure 8.

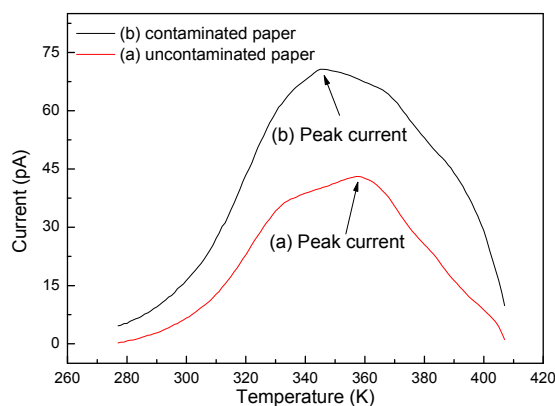


Figure 8. Thermally stimulated current (TSC) test results of two insulation paper samples: (a) uncontaminated paper; (b) contaminated paper.

The current peak related to trap energy level in sample II (contaminated by copper sulfide) shifted to a lower temperature compared with that in sample I (from 356 K to 344 K). This phenomenon indicated that shallower trap levels were generated in contaminated paper. Trapped charges and trap levels were calculated to analyze the trap characteristics. The trap charge amounts Q_{tsc} and the trap level E could be calculated according to the TSC test results using the following equations:

$$Q_{\text{tsc}} = \int_{t_0}^{t_1} I(t) dt = \frac{60}{\beta} \int_{T_0}^{T_1} I(T) dT \quad (2)$$

$$E = \frac{2.47 T_m^2 k}{\Delta T} \quad (3)$$

where T_m is the corresponding temperature to the peak current (K); β is the heating rate (K/min); ΔT is the temperature difference from the peak current to the half peak current (K); and k is the Boltzmann constant. Table 5 shows the TSC parameters of two paper samples.

Table 5. Thermally stimulated current (TSC) test results.

Parameter	Sample I	Sample II
Peak current (pA)	42.891	68.995
Temperature of peak current (K)	356	344
Trapped charges (nC)	0.546	0.912
Trap levels (eV)	0.819	0.476

As shown in Table 5, the trap level of contaminated paper was 0.476 eV, which is lower than that of uncontaminated paper (0.819 eV). Nevertheless, the trap charge amount of contaminated paper showed opposite characteristics (higher than that of uncontaminated paper). Lower trap level and higher trap charge amounts indicated that numerous shallower traps were present in contaminated paper. Furthermore, the shallower trap level could accelerate the de-trapping velocity of trapped electrons, leading to a more frequently charged transport. Therefore, electrons could easily accumulate energy and become thermion because of the decrease in trap levels. Electric tree and discharge channels formed easily. Excessive amounts of shallower traps also had an adverse effect on the anti-aging properties of insulation paper. However, the current peak, which was connected to the maximum trap density for contaminated paper was higher than that of uncontaminated paper, indicating that contaminated paper possessed higher trap density. These findings resulted in high-speed charge transportation via de-trapping and trapping processes in shallower traps.

5. Conclusions

This paper presents the space charge behavior in insulation paper induced by copper sulfide in HVDC power transformers. SEM, PEA, and TSC methods were used to conduct corresponding experiments and analyses. The results of the reported work and analyses are summarized as follows:

- (1) The electrical insulating characteristics of paper material contaminated by copper sulfide decreased largely because of its semi-conductor properties.

(2) Copper sulfide on paper not only enhanced charge accumulation but also improved the mobility of the charge in the paper materials.

(3) The space charge behaviors of the thermally aged paper materials before and after contamination demonstrated that shallower trap energy level and higher trap density were generated because of the introduction of copper sulfide. These two reasons directly led to the rapid transfer of charge carriers via de-trapping and trapping processes. This phenomenon may explain why dielectric strength and breakdown voltage of aged paper materials contaminated by copper sulfide decreased compared with uncontaminated paper.

Acknowledgments

The authors acknowledge the National Natural Science Foundation of China (51277187) with supporting this research.

Author Contributions

All authors contributed extensively to the work presented in this paper. Ruijin Liao supervised the project. Ende Hu conducted the detail experiments and measurements. Lijun Yang and Yuan Yuan performed profiles and results analysis. All authors discussed the results and implications and commented on the manuscript at all stages.

Conflicts of Interest

The authors declare no conflict of interest.

References

1. Okabe, S.; Kohtoh, M.; Amimoto, T. Investigation of electrostatic charging mechanism in aged oil-immersed transformers. *IEEE Trans. Dielectr. Electr. Insul.* **2011**, *17*, 287–293.
2. Saha, T.K. Review of time-domain polarization measurements for assessing insulation condition in aged transformers. *IEEE Trans. Dielectr. Electr. Insul.* **2003**, *18*, 1293–1301.
3. Blaise, G. Space charge physics and the breakdown process. *J. Appl. Phys.* **1995**, *77*, 2916–2927.
4. Wang, X.; Yoshimura, N.; Murata, K.; Tanaka, Y.; Tanaka, T. Space charge characteristics in polyethylene. *J. Appl. Phys.* **1998**, *84*, 1546–1550.
5. Scatiggio, F.; Tumiatti, V.; Maina, R.; Tumiatti, M.; Pompili, M.; Bartnikas, R. Corrosive sulfur induced failed in oil-filled electrical power transformers and shunt reactors. *IEEE Trans. Power. Deliv.* **2009**, *24*, 1240–1248.
6. De Carlo, R.M.; Bruzzoniti, M.C.; Sarzanini, C.; Maina, R.; Tumiatti, V. Copper contaminated insulating mineral oils-testing and investigation. *IEEE Trans. Dielectr. Electr. Insul.* **2013**, *20*, 557–563.
7. Martins, M.A.G.; Gomes, A.R.; Pahlavanpour, B. Experimental study of passivated oil corrosiveness after depletion of the passivator. *IEEE Electr. Insul. Mag.* **2009**, *25*, 23–27.
8. Bolliger, D.; Pilania, G.; Boggs, S. The effect of aromatic and sulfur compounds on partial discharge characteristics of hexadecane. *IEEE Trans. Dielectr. Electr. Insul.* **2013**, *20*, 801–813.

9. Rajan, J.S.; Rudranna, N. Electric stress distribution in paper oil insulation due to sulphur corrosion of copper conductors. *J. Electrostat.* **2013**, *71*, 429–434.
10. Liao, R.; Guo, C.; Wang, K.; Yang, L.; Grzybowski, S.; Sun, H. Investigation on thermal aging characteristics of vegetable oil-paper insulation with flowing dry air. *IEEE Trans. Dielectr. Electr. Insul.* **2013**, *20*, 1649–1658.
11. Ahmed, N.H.; Srinivas, N.N. Review of space charge measurements in dielectrics. *IEEE Trans. Dielectr. Electr. Insul.* **1997**, *4*, 644–656.
12. Tang, C.; Chen, G.; Fu, M.; Liao, R.J. Space charge behavior in multi-layer oil-paper insulation under different DC voltage and temperatures. *IEEE Trans. Dielectr. Electr. Insul.* **2010**, *17*, 775–780.
13. Du, Y.; Lv, Y.; Li, C.; Chen, M.; Zhou, J.; Li, X.; Tu, Y. Effect of electron shallow trap on breakdown performance of transformer oil-base nanofluids. *J. Appl. Phys.* **2011**, *110*, doi:10.1063/1.3660783.
14. Toyama, S.; Tanimura, J.; Yamada, N.; Nagao, E.; Amimoto, T. Highly sensitive detection method of dibenzyl disulfide and the elucidation of the mechanism. *IEEE Trans. Dielectr. Electr. Insul.* **2009**, *16*, 509–515.
15. Rudranna, N.; Rajan, J.S. Modeling of copper sulphide migration in paper oil insulation of transformers. *IEEE Trans. Dielectr. Electr. Insul.* **2012**, *19*, 1642–1649.
16. Kawarai, H.; Uehara, Y.; Mizuno, K.; Toyama, S.; Nagao, E.; Hosokawa, N.; Amimoto, T. Influences of oxygen and 2, 6-di-tert-butyl-p-cresol on copper sulfide deposition on insulating paper in oil-immersed transformer insulation. *IEEE Trans. Dielectr. Electr. Insul.* **2012**, *19*, 1884–1890.
17. Maina, R.; Tumiatti, V.; Pompili, M.; Bartnikas, R. Corrosive sulfur effect in transformer oil and remedial procedures. *IEEE Trans. Dielectr. Electr. Insul.* **2009**, *16*, 1655–1663.
18. Chong, Y.L.; Chen, G.; Miyake, H.; Matsui, K.; Tanaka, Y.; Takada, T. Space charge and charge trapping characteristics of cross-linked polyethylene subjected to ac electric stresses. *J. Phys. D Appl. Phys.* **2006**, *39*, 1658.
19. Huang, X.; Jiang, P.; Yin, Y. Nanoparticle surface modification induced space charge suppression in linear low density polyethylene. *Appl. Phys. Lett.* **2009**, *95*, doi:10.1063/1.3275732.
20. Hao, J.; Chen, G.; Liao, R.; Yang, L.; Tang, C. Influence of moisture on space charge dynamics in multilayer oil-paper insulation. *IEEE Trans. Dielectr. Electr. Insul.* **2012**, *19*, 1456–1464.